T. Magn. Soc. Jpn. (Special Issues)., **1**, 61-65 (2017)

<Paper>

# Estimation of eddy current loss for transformer windings based on RNA

T. Hiwatashi, K. Tajima, and Y. Yoshida*

Department of Cooperative Major in Life Cycle Design Engineering, Akita Univ., *1-1, Tegata Gakuen-machi, Akita 010–5802, Japan*

*Department of Electrical and Electronic Engineering, Akita Univ., *1-1, Tegata Gakuen-machi, Akita 010–5802, Japan*

An estimation method of eddy current loss for transformer windings based on reluctance network analysis (RNA) is proposed. As the initial stage of study, the authors focus on eddy current loss occurring in the transformer windings and configured a simple evaluation model to estimate eddy current loss in prism copper wires simulating transformer windings. The validity of the proposed method is demonstrated by comparing 3D-FEA and experimental results.

**Keywords:** DC-DC converter, reluctance network analysis (RNA), eddy current loss, transformer winding

## 1. Introduction

DC-DC converters have been used mainly as the DC-power sources of electronic equipment. With the growing demand for compact, high-efficiency electric equipment, DC-DC converters are now also required to be compact and high-efficiency. Magnetic devices occupy a large volume in DC-DC converters, and the size of these devices has been reduced by higher switching frequency. However, higher switching frequency increases the switching loss. A common method for switching loss reduction is zero voltage switching (ZVS). Further, it is well known that transformer cores have a gap in some cases, and leakage fluxes have increased due to gaps in the transformer core[1]. The leakage of magnetic fluxes interlinking with the transformer winding is what causes the eddy current flow and loss inside the windings. For the transformer, in order to design based on complex high-frequency magnetic flux distribution and current density distribution, a simulation technique having high accuracy and requiring a short period of time for calculation is needed.

Reluctance network analysis (RNA) has proven effective for the design of magnetic devices such as motors and inductors[2),3)]. In addition, since it is possible to perform calculations by general circuit simulation software such as SPICE, coupled analysis of the electric circuit and magnetic devices such as a DC-DC converter is possible and can be expected to serve as a highly practical design technique.

The authors previously studied how to estimate eddy current loss caused by the leakage magnetic flux for transformer windings based on simple assumptions[4]. In this paper, as the initial stage of study, the authors focus on eddy current loss occurring in the transformer windings and configured a simple evaluation model to estimate eddy current loss in prism copper wires simulating the transformer windings. The validity of the proposed model is demonstrated by comparing 3D-FEA and experimental results.

## 2. Analysis model

### 2.1 Specifications of the analysis object

Figure 1 shows the shape and specifications of the analytical and experimental object used in the consideration. The exciting coils are wound around U-shape cores. A total of six prism copper wires sized 2.0 mm × 2.0 mm × 20 mm are sandwiched by the ferrite cores. The number of winding turns of the exciting coils per leg and the depth of the cores and prism copper wires are five turns and 20 mm, respectively.

### 2.2 Derivation of the RNA model

The schematics of the three dimensional (3D) RNA model are shown in Fig. 2. Figure 2(a) gives an overview of the magnetic circuit. $Ni$ are magnetomotive forces (MMF), $R_{\mathrm{mcore}}$ are the magnetic reluctances of the core, and $R_{\mathrm{mLcoil}}$ and $R_{\mathrm{mLgap}}$ are the reluctances of leakage magnetic flux path in the exciting coils and the gaps. The gaps are divided, as shown in Fig. 2(b). The air gaps between the core and a prism copper wire are divided into fine elements with a size of 0.2 mm × 0.2 mm and the other area around the air gap is divided with a size of 2.0 mm × 0.2 mm or 2.0 mm × 0.25 mm. In order to accurately represent the flow of the magnetic flux of the gaps, prism copper wires are divided into fine elements with a size of 0.2 mm × 0.25 mm. The skin effect is considered in this division. Generally, skin depth $\delta$ of the conductor is obtained from

$$\delta = \sqrt{\frac{2\rho}{\omega\mu}}, \qquad (1)$$

where $\rho$ is resistivity of the conductor, $\omega$ is angular frequency, and $\mu$ is permeability of the conductor. Skin

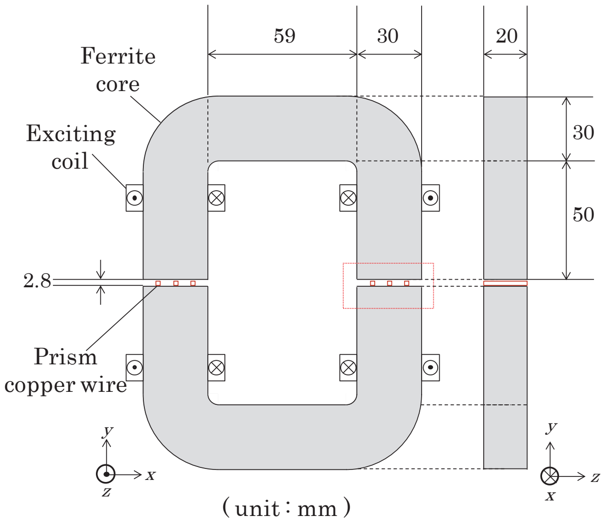


(a) General view of analysis model

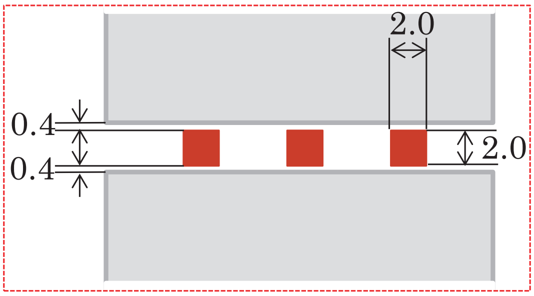


(b) Enlarged view of the gap

**Fig. 1** Specifications of analysis object.

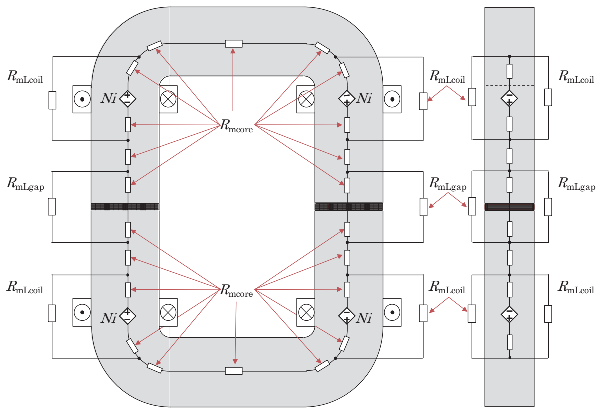

(a) Overview of magnetic circuit

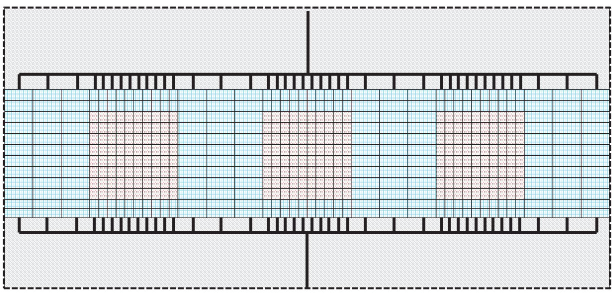

(b) Division of gap

**Fig. 2** Schematics of 3D-RNA model.

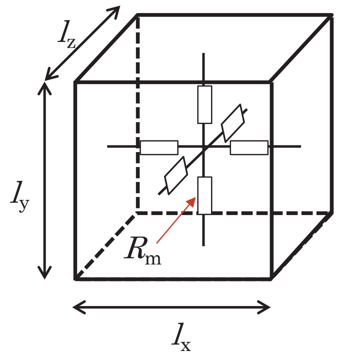


**Fig. 3** Unit magnetic circuit.

depth of a prism copper wire is about 0.65 mm in frequency at 10 kHz and $\rho$ = 1.673×10$^{-8}$ Ωm (at 20 degrees Celsius), so prism copper wires are assumed to be affected by the skin effect. Therefore, the prism copper wires are divided by 0.2 mm in the *x*-axis direction and by 0.25 mm in the *y*-axis direction.

Each divided element is expressed in a 3D unit magnetic circuit. Figure 3 shows the unit magnetic circuit of the prism copper wire and the air region. In the figure, $l_x$, $l_y$, and $l_z$ are the lengths of the element. The reluctance $R_m$ in the unit magnetic circuit is obtained from

$$R_m = \frac{l_y}{2\mu_0\mu_r(l_x \times l_z)}, \qquad (2)$$

where $\mu_0$ is permeability of the vacuum and $\mu_r$ is relative permeability. By connecting all unit magnetic circuits together, the RNA model is obtained.

In the proposed model, the relative permeability of the core, the prism copper wires, and the air region are set to 2300, 1, and 1, respectively.

Figure 4 shows the magnetic circuit of a prism copper wire and MMFs. Figure 4(a) shows the front view of a prism copper wire and (b) shows the dotted frame part of Fig. 4(a). When magnetic flux $\phi_{11}$ flows to one element of a prism copper wire, the electromotive force by Faraday's law causes eddy current $i_{11}$ occur. Eddy current $i_{11}$ produces an MMF in the magnetic circuit, as shown in Fig. 4(b). Similarly, $\phi_{21}$ affected by the MMF flows to the element below. Thus, the skin effect can be taken into account by placing the MMFs in the *y*-axis direction.

Figure 5 shows the division of the *z*-axis direction of a prism copper wire. In order to consider the eddy current distribution accurately, a prism copper wire is divided into 10 splits in the *z*-axis direction. The tip of the wire is divided by 0.2 mm.

Figure 6(a) shows the electric circuits of a prism copper wire. Eddy currents calculated by the four-layer independent electric circuit can be converted into the MMFs in the magnetic circuit, as shown in Fig. 4. When the magnetic flux in the electrical circuit of a certain element flows, the electromotive force $d\phi/dt$ occurs due to Faraday's law. Eddy current $i$ is calculated by the electromotive force and the electric resistances of the elements. Each divided element is expressed in a unit

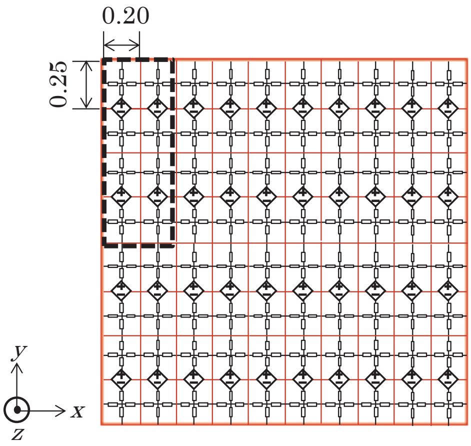


(a) Front view of a prism copper wire

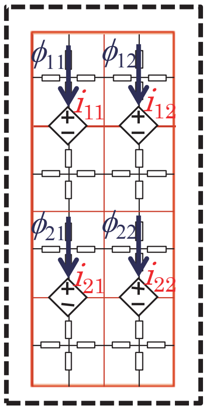


(b) Part of the enlarged view

**Fig. 4** Magnetic circuit of a prism copper wire and magnetomotive force.

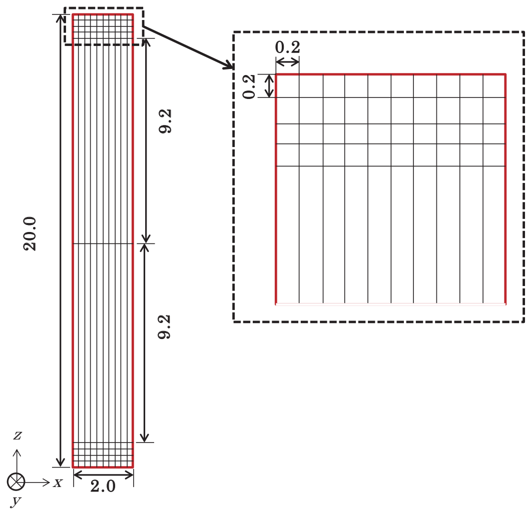


**Fig. 5** Division of z-axis direction of a prism copper wire.

electric circuit, as shown in Fig. 6(b). The resistances $r_x$ and $r_z$ in the unit electric circuit are obtained from

$$r_x = \rho \frac{2\Delta x}{\Delta y \Delta z}, \quad (3)$$

$$r_z = \rho \frac{2\Delta z}{\Delta x \Delta y}, \quad (4)$$

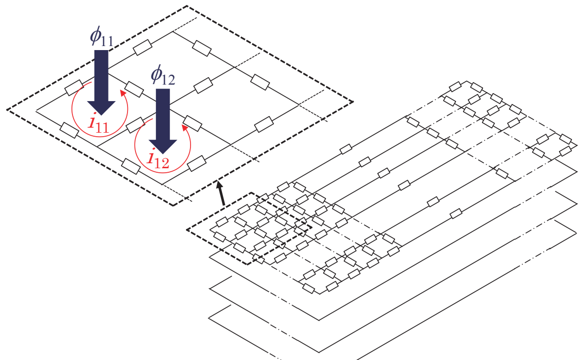


(a) Electric circuit of a prism copper wire

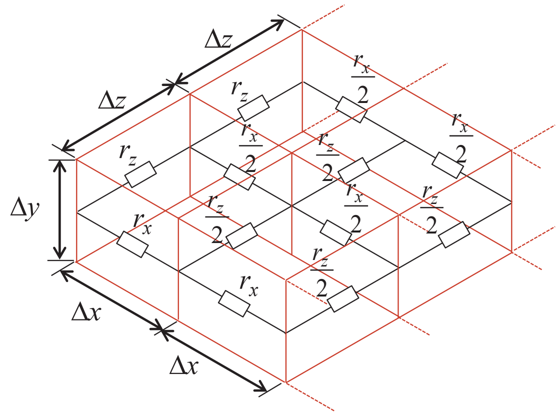


(b) Electric resistances of circuit

**Fig. 6** Electric circuit of a prism copper wire and the electric resistances.

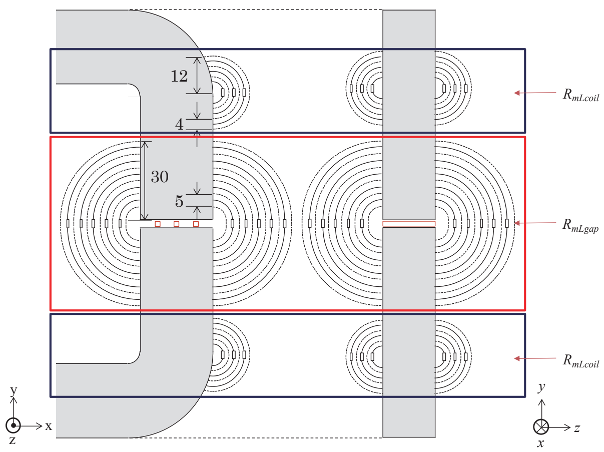


**Fig. 7** Setting method of the reluctance of leakage magnetic flux path in exciting coil and the gap.

where $\Delta x$ is the element length in the $x$-axis direction, $\Delta y$ is the element length in the $z$-axis direction, and $\Delta z$ is the element length in the $z$-axis direction, respectively. If there is an adjacent element, the resistance in the circuit becomes halved because the two adjacent resistances are connected in parallel.

Figure 7 shows the setting method of the reluctances of leakage flux paths in the exciting coils and the gaps. At high frequency, the quantity of leakage of the magnetic flux is expected to be greater than at by

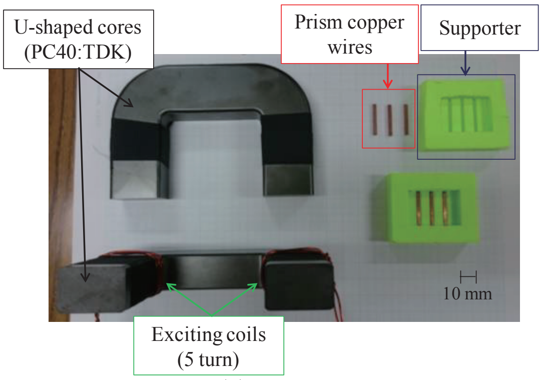


(a) Exposed view

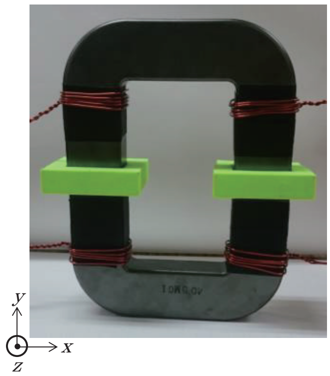


(b) Assembled set-up

**Fig. 8** Photographs of experimental apparatus.

low frequency. In this paper, the leakage magnetic paths in the $x$-axis direction and the $z$-axis direction are approximated straight lines (gap length) and arcs to represent the leakage magnetic flux. The leakage magnetic flux paths around the exciting coils are approximated by only arcs. Further, reluctances are connected in parallel with the magnetic flux path flow to the main magnetic flux such that the leakage magnetic flux paths are combined into a single path, as shown in Fig. 2(a).

## 3. Comparison with experimental results

To verify the calculation accuracy of the RNA model, the calculated values were compared to the measured ones. Figure 8 shows a photograph of the experimental apparatus, where (a) is an exposed view. U-shaped cores are made of ferrite (PC40, TDK). Supporters (PLA resin) are sandwiched between the cores to fix the positions of the cores and the prism copper wires. Figure 8(b) shows the assembled experimental set-up and Fig. 9 shows the configuration of experimental set-up. Bipolar power supply (PBZ40-10, KIKUSUI) was used for the power supply. Excited voltage $v_e$ and current $i_e$ are measured with a power meter (2533E, YOKOGAWA). The sum of iron loss in the core, copper loss in the exiting coils, and eddy current loss in the prism copper wires $W_{total}$ is given by

$$W_{total} = \frac{1}{T}\int_1^T v_e i_e dt \,. \tag{5}$$

To extract eddy current loss occurring in the prism copper wires, the method shown in Fig. 10 was adopted.

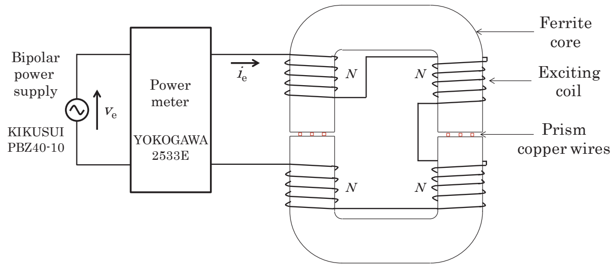


**Fig. 9** Configuration of experimental set-up.

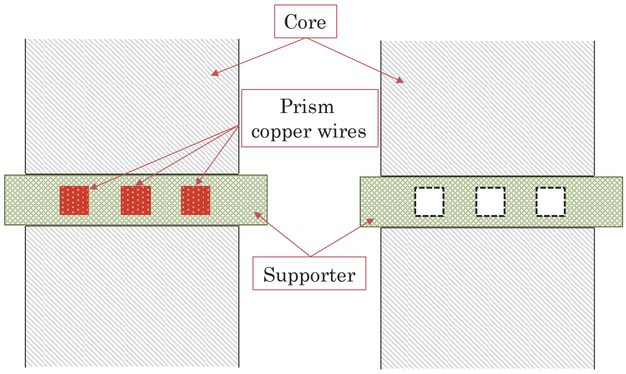


**Fig. 10** Extraction methods of eddy current loss occurring in the prism copper wires: (a) case of prism copper wires being sandwiched and (b) case of only the supporter being sandwiched.

Figure 10(a) shows the case of prism copper wires being sandwiched. In this case, occurring total loss $W_A$ is given by

$$W_A = W_i + W_c + W_e \,, \tag{6}$$

where $W_i$ is iron loss in the core, $W_c$ is copper loss of the exciting coil, and $W_e$ is eddy current loss of the prism copper wires. Figure 10(b) shows a case without the prism copper wires, where occurring loss $W_B$ is given by

$$W_B = W_i' + W_c' \,. \tag{7}$$

For both loss measurements, the exciting current was sine wave at 4.0 A root-mean-square value constant and same frequency. Therefore, copper loss $W_c$ and $W_c'$ were equal. Iron loss $W_i$ was not equal to $W_i'$ because the prism copper wires were sandwiched. However, since the ferrite core was used, the iron loss itself was smaller than the eddy current loss of the prism copper wires, so the difference between $W_i$ and $W_i'$ was ignored in this paper. Thus, eddy current loss $W_e$ in the prism copper wires is given by

$$W_e = W_A - W_B \,. \tag{8}$$

Figure 11 shows the experimental results of loss measurement and the calculation results in 3D-FEA. The exciting current was sine wave at 4.0 A root-mean-square value constant, and the frequencies of the exciting current were 1, 3, 5, 8, and 10 kHz. Copper loss of the exciting coil in the experiment was obtained from the product of the square of effective value of excited current and DC resistance ($R_{DC}$ = 0.086 Ω) in the exciting coil. Since the excited current was constant for each frequency, copper loss was almost constant. Iron loss in the core obtained by 3D-FEA tended to increase with frequency. Since there was almost no difference in iron loss with and without the prism

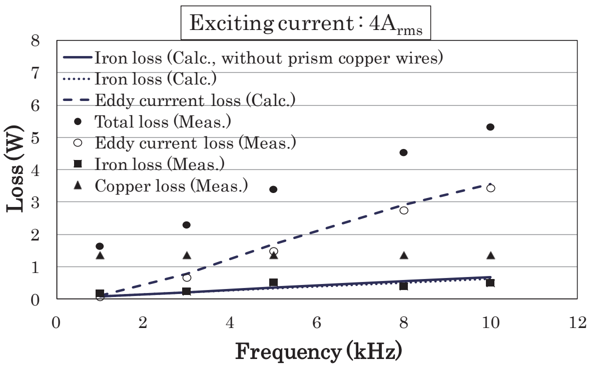


**Fig. 11** Experimental results of loss measurement and calculation results in 3D-FEA.

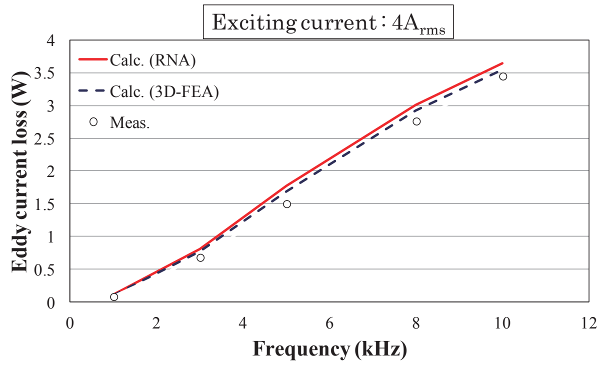


**Fig. 12** Comparison of eddy current loss in prism copper wires obtained from proposed model, experiment, and 3D-FEA.

copper wires, the validity of the experimental method was confirmed. Measured values and calculation values of iron loss showed similar tendencies, but there were some discrepancies. These discrepancies were considered to be due to experimental error. Since the eddy current loss occurring in the prism copper wires is subtracted the sum of iron loss and copper loss from total loss as determined from equation (8), it is considered that the measurement error of iron loss directly affected the difference in eddy current loss.

Figure 12 shows the relationship between eddy current loss of the prism copper wires and frequency. Calculating conditions were the same as those in Fig. 11. As seen in the figure, the calculated values obtained from the proposed RNA model were in almost perfect agreement with the ones obtained from the experiment and 3D-FEA.

The validity of the division of a prism copper wire was confirmed by current density distribution. Figure 13 shows the current distributions of RNA and 3D-FEA in the exciting current at maximum and frequency at 10 kHz.

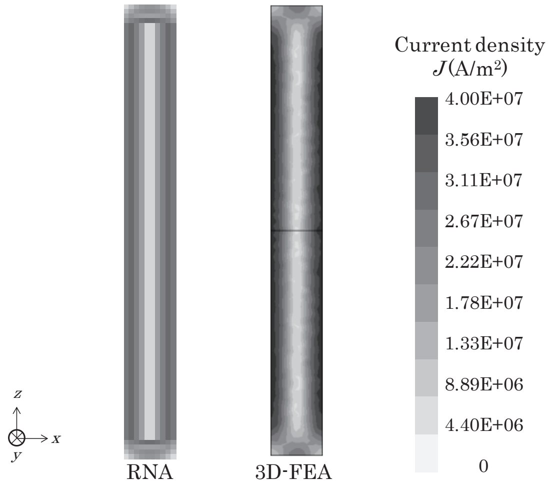


**Fig. 13** Comparison of current density distribution in a prism copper wire in exciting current at maximum and frequency at 10 kHz.

The prism copper wire was chosen to be sandwiched in the middle of the right leg in Fig. 1. Both current density distributions show a similar tendency, which demonstrates that skin effect can be considered in the proposed model.

## 4. Conclusion

An estimation method of eddy current loss in prism copper wires based on RNA was proposed. The usefulness of the proposed method was demonstrated by comparisons with the FEA and an experiment. Further studies will attempt to estimate eddy current loss for transformer windings in a DC-DC converter by using the proposed method.

## References

1) T. Ninomiya, *IEEJ Trans. IA*, **117**, 2, 120 (1997).
2) K. Tajima and T. Sato, *J. Magn. Soc. Jpn.*, **34**, 3, 367 (2010).
3) K. Nakamura, K, Honma, T. Ohinata, K. Arimatsu, T. Shirasaki, and O. Ichinokura, *J. Magn. Soc. Jpn.*, **38**, 4, 174 (2014).
4) T. Hiwatashi, K. Tajima, and Y. Yoshida, The papers of Technical Meeting on Magnetics, *IEE Jpn*, MAG-16-035 (2016).

**Received Oct. 10, 2016; Revised Dec. 9, 2016; Accepted Mar. 4, 2017**